Journal of Alloys and Compounds 586 (2014) S143–S149

Contents lists available at SciVerse ScienceDirect

Journal of Alloys and Compounds

journal homepage: www.elsevier.com/locate/jalcom

Experimental investigation of diffusion behavior between molten Mg and Nd–Fe–B magnets

Hong Jun Chae [a,b], Young Do Kim [b], Bum Sung Kim [a], Jeong Gon Kim [c], Taek-Soo Kim [a,*]

[a] Korea Institute of Industrial Technology, 7-47, Songdo-dong, Yeonsu-gu, Incheon 406-840, Republic of Korea
[b] Hanyang University, 17, Hengdang-dong, Sungdong-gu, Seoul 133-791, Republic of Korea
[c] Incheon University, 12-1, Songdo-dong, Yeonsu-gu, Incheon 406-772, Republic of Korea

ARTICLE INFO

Article history:
Available online 14 March 2013

Keywords:
Nd–Fe–B
Recycling
Liquid metal extraction
Rare-earth elements
Neodymium

ABSTRACT

This study presents the experimental results of neodymium (Nd) extraction from the Nd–Fe–B magnetic alloy by liquid magnesium (Mg). A sample of Nd–Fe–B alloy was placed in an Fe crucible with pure Mg under an Ar atmosphere and melted by induction heating. In order to identify the reaction mechanism, the effects of melting temperature (993–1073 K) and holding time (2–120 min) on the extraction ability were investigated. The diffusion behavior was analyzed by scanning electron microscopy (SEM) and energy dispersive spectroscopy (EDS) and the constituent phases were characterized by X-ray diffraction (XRD). It was found that Nd from the Nd–Fe–B alloy diffused readily into liquid Mg. The reaction rate was dependent both on temperature and time. This study demonstrates that liquid metal extraction of Nd could be a viable and inexpensive method for recovery of the expensive rare earth element Nd using Mg castings.

1. Introduction

In recent years, Nd–Fe–B magnetic materials have emerged as the leaders in high-field permanent magnet applications. They exhibit the highest energy product of all permanent magnets and possess excellent resistance to demagnetization at normal operating temperatures. Nd–Fe–B magnets have become widespread in automotive cranking motors, computers, audio-visual components, magnetic separators, military, aerospace systems, and other devices that require high-field magnets of small size or weight [1–3]. The production of Nd–Fe–B magnets consistently increases by about 20% per year because of their excellent magnetic properties. However, the expansion of the Nd–Fe–B magnet market has made the natural scarcity of Nd a concern for many researchers. The development of an effective recycling process for Nd–Fe–B magnet scraps is thus an extremely important issue from the resource and energy conservation viewpoint. Several recycling processes have been reported for the rare-earth elements in Nd–Fe–B magnets [4–6]. It has been proposed that the best separation of rare-earths from the Nd–Fe–B magnets can be obtained by sulfuric acid dissolution followed by precipitation of the recyclable rare-earth salts. However, this process is disadvantageous because of its tendency to create large amounts of waste water, including some dangerous compounds. In order to avoid this issue, Xu et al. have reported a technique to extract Nd from 18Nd–72.4Fe–0.9B–1.82Pr–5.3Dy (wt.%) magnet scraps using liquid metal extraction (LME) processing [7,8]. However, these techniques are difficult to apply because the primary reaction mechanism between Mg and Nd–Fe–B scrap is unclear. In order to identify the specific reaction mechanism, a diffusion couple consisting of an Nd magnet and Mg was prepared. The effects of melting temperature and time on the diffusion properties of Mg and Nd–Fe–B alloys were investigated to determine if these LME methods could be used in industrial applications.

2. Experimental procedures

The selective extraction behavior of Nd from Nd–Fe–B scrap by molten Mg was investigated. The Nd–Fe–B magnet starting material for this experiment was supplied by the JAHWA electronics Co. Ltd., Republic of Korea. Pure Mg (purity: 99.99%) was purchased from at Canada (JC magnesium). The chemical compositions of the Nd–Fe–B magnet shown in Table 1 were determined by an inductively coupled plasma mass spectrometry (ICP-MS, Model NexION 300, Perkinelmer Korea). The initial Nd–Fe–B magnet and pure Mg were designed to be $10 \times 10 \times 5$ mm and $10 \times 10 \times 10$ mm, respectively. To make the diffusion couples, the Nd–Fe–B magnets were first placed in a mild steel crucible with Mg and induction heated with a 20 KW DTIH-0020VMF generator in an atmosphere-controlled chamber to the proper temperature (993–1073 K) and time range (2–120 min) in Ar atmosphere. The temperature was monitored continuously with a thermocouple. Before heating, the crucible was covered with quartz pipe and Ar shielding gas (purity: 99%+) to minimize oxidation and Mg vaporization.

For analyzing the characteristics of the Nd–Fe–B magnet obtained by slow cooling at air atmosphere it according to changes in times for each given temperature, the magnet was cut into proper sized specimens using a diamond wheel with a thickness of 0.3 mm and the specimens were grinded using abrasive papers scaled

* Corresponding author. Tel.: +82 32 8500 409; fax: +82 32 8500 390.
E-mail addresses: hjchae@kitech.re.kr (H.J. Chae), ydkim1@hanyang.ac.kr (Y.D. Kim), bskim15@kitech.re.kr (B.S. Kim), jyj309@incheon.ac.kr (J.G. Kim), tskim@kitech.re.kr (T.-S. Kim).

0925-8388/$ - see front matter © 2013 Elsevier B.V. All rights reserved.
http://dx.doi.org/10.1016/j.jallcom.2013.02.156

Table 1
Overall composition of Nd–Fe–B magnet (wt.%).

Nd	Dy	Co	Cu	Al	Nb	B	Fe
24.43	8.14	1.67	0.15	0.2	0.37	0.97	64.07

from 200 grit SiC to 2000 grit SiC. Then, the specimens were finally finished using 0.3 μm Al_2O_3 suspension. After polishing the specimens, the specimens were cleaned in an ultrasonic unit for 5 min by steeping them in ethanol. Then, the specimens were returned after drying them using a high pressure air spray gun. The thickness of the diffusion layer in the Nd–Fe–B magnet was measured using SEM and the concentrations of the Nd and Mg in the diffusion layers were investigated using ICP-MS and EDS analyses.

3. Results and discussion

3.1. Reaction model between the solid Nd–Fe–B magnet and the liquid Mg

Fig. 1 shows the cross-section of the Nd–Fe–B specimen after melting it using a high frequency induction process in which the object positioned at the bottom of the crucible was the Nd–Fe–B magnet and the Mg was solidified at the upper section.

Fig. 2 shows the SEM microstructure of Nd–Fe–B magnet (a) and pure Mg (b), and XRD traces characterized from Nd–Fe–B (c) and pure Mg (d). Combining both the results, the Nd contained alloy consists of $Nd_2Fe_{14}B$ (described as 2) and Nd-rich phases (described as 1). Here, the $Nd_2Fe_{14}B$ phases showed a polygon shape, and the Nd-rich phase is formed along the grain boundaries and the boundary intersection point.

In order to identify the compositional variation in the Nd–Fe–B magnets, EDS was performed on both the grains and the grain boundaries and the results are listed in Table 2. They indicate that the Nd is concentrated in the grain boundaries rather than within the grains.

3.2. Microstructure of diffusion region in the Nd–Fe–B magnet

Fig. 3I shows the microstructures of the interface between Nd–Fe–B magnet and Mg cast at 993 K for various lengths of time between 2 and 120 min. Based on the images, the diffusion distance was proportional to temperatures and maintaining times and exhibited a linearly increased behavior. This phase transformation study concerns those mechanisms by which a system attempts to reach this state and how long it takes. One of the most fundamental processes that controls the rate at which many transformations occur is atomic diffusion, which is always driven by decreases in Gibbs free energy. In this case, a decrease in free energy is produced by Nd and Mg atoms diffusing from regions of high concentration to those of low concentration [9]. Thus, the Nd–Fe–B specimen was divided into two parts: a diffusion zone and an unaffected zone. In addition, the variation in diffusion layer thickness of the cast samples was plotted in Fig. 3II as a function of melting temperature in the 993–1073 K range. The diffusion layer cast at 993 K for 2 min was approximately 6 μm wide. The thickness increased to 42 μm, 120 μm, 229 μm, 298 μm, 365 μm, 460 μm, 610 μm, 870 μm, 1037 μm, 1200 μm and then 1630 μm for holding times of 5 min, 10 min, 20 min, 30 min, 40 min, 50 min, 60 min, 70 min, 80 min, 90 min and 120 min, respectively. The diffusion layer thickness rapidly increased over 120 min from 137 to 1946 μm and 250 to 2416 μm when cast at 1023 and 1073 K, respectively. The mean diffusion velocity is dependent on temperature, leading to the increase in diffusion layer thickness observed with increasing temperature.

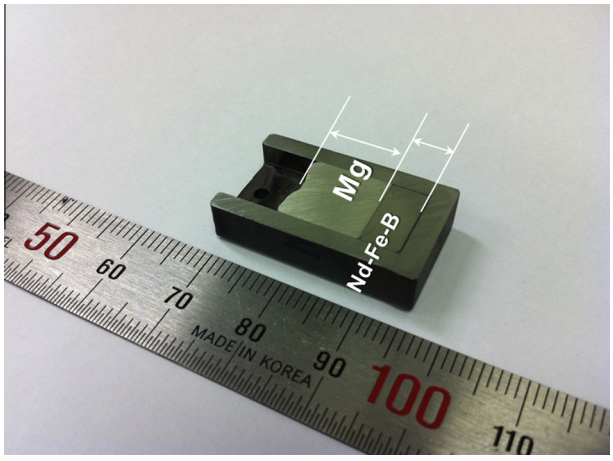

Fig. 1. Macrostructure of a typical cast sample.

Fig. 4I shows a series of high-magnification micrographs which illustrates the phases present in the various regions between the unaffected Nd–Fe–B and the solidified Mg layers. Close observation of the sample by backscattered electron (BSE) imaging reveals that the Nd–Fe–B consists of four distinct phases. The compositions of these phases are detailed in Table 3. Boron was not reported in this study because the element could not be detected reliably. The identifications made in Table 3 are based on the relative detected amounts of Nd and Fe and the phases known to commonly exist in Nd–Fe–B magnet materials [10]. Based on this analysis, the white phase at the grain boundaries of the Nd–Fe–B magnet and marked "1" in Fig. 4a is identified as Nd(Dy)-rich, while the gray matrix "2" is a $Nd_2Fe_{14}B$ phase. In the transition regions shown in Fig. 4b and c, a Nd-depleted region exists where Nd has diffused from the Nd–Fe–B magnet. The same phases are observed in this region, namely, $Nd_2Fe_{14}B$, Nd(Dy)-rich and α-Fe + Transition metal + pure Mg, although now Fe + Nd(Dy)-rich is the dominant phase in the diffusion layer. The diffusion layer–Mg interface is shown in Fig. 4d. The major phase is α-Fe + Nd(Dy)-rich. A few small light particles can be seen near the interface but within the α-Fe + Nd(Dy)-rich diffusion zone. The composition abruptly changes at the interface as the now-solidified Mg becomes the matrix phase. The microstructure of the solidified Mg consists of dendrite-like equiaxial Mg grains with Nd-rich intermetallic phases present at the grain boundaries. EDS analysis showed that the matrix contains Nd in solid solution in amounts up to 2.01 wt.%. The phase on the grain boundaries contains 36.7 wt.% Nd and it is identified as $Mg_{12}Nd$. The Mg–Nd phase diagram predicts that upon cooling, $Mg_{12}Nd$ will precipitate from a supersaturated solid solution [11]. These macroscopic results confirm that Nd in Nd–Fe–B magnets can be selectively extracted by liquid Mg.

3.3. Microstructure of the solidified Mg matrix

Fig. 5 shows the panoramic change of microstructures in Mg zone according to distances based on the interface of the sample, reacted at 993 K for 20 min, and the EDS analysis results at the point (1) and (2). In order to know the element distribution EDS mapping are also conducted for Fe, Nd and Mg. It is seen that the reaction between the liquid Mg and solid Nd–Fe–B results in forming Mg–Nd dendritic compounds within the α-Mg matrix. The interface between the Nd–Fe–B and solidified Mg is covered with a thin layer of homogeneous Nd-rich (a). The thickness of the boundary layer in the liquid Mg at the interface (δ) value was set at 10 μm (1). From the microstructure, it appears that the high affinity of Mg for Nd causes Nd to rapidly diffuse out of the Nd–Fe–B magnet and into the liquid Mg, forming the $Mg_{12}Nd$ phases